PRAMANA
— journal of
physics

© Indian Academy of Sciences

Vol. 81, No. 3
September 2013
pp. 535–545

Low-limit detection of NO_2 by longitudinal mode selection in a photoacoustic resonant system

F YEHYA and A K CHAUDHARY*
Advanced Centre of Research in High Energy Materials, University of Hyderabad, Hyderabad 500 046, India
*Corresponding author. E-mail: anilphys@yahoo.com

MS received 1 December 2012; accepted 11 June 2013

Abstract. The paper reports the pulsed laser-based photoacoustic (PA) spectroscopy of NO_2 in a resonant PA cavity with special filters made of stainless steel. The PA cell along with special types of sound filters are designed and fabricated to excite only the second-order longitudinal mode inside the cavity. The second harmonic, i.e. $\lambda = 532$ nm pulse width, of 7 ns obtained from Q-switched Nd:YAG laser at 10 Hz repetition rate has been used to study the saturation behaviour of the PA signal and absorption coefficient with respect to the input laser energy. Generally, the Q-factor of longitudinal modes in the acoustic cavities is quite low. However, by modifying the design of the cell and the filter, we can achieve high value of $Q = 30$. The combination of special filter along with the experimental data acquisition technique helped us to achieve the minimum detection concentration of NO_2 of the order of 9 ppbV which is much better than the previous value of the same PA cell without filter [Yehya and Chaudhary, *Appl. Phys. B* **106**, 953 (2012)].

Keywords. Photoacoustic; pulsed laser; second longitudinal mode; filters; NO_2.

PACS No. 78.20.hb

1. Introduction

Photoacoustic spectroscopy is one of the most popular and efficient absorption techniques. It is mainly used for detecting different types of atmospheric pollutants at trace level. The ultimate detection sensitivity of the PA sensor depends on several factors such as the stored heat energy in the absorbed sample, input laser power, nature of the gas sample, cell constant and microphone sensitivity [1–3]

NO_2 is one of the atmospheric pollutant gases emitted from automobile exhausts, industrial boilers, electrical power generators and high-energy materials. It is responsible for breathing and bronchial problems. Moreover, its oxidation affects the ozone cycle in the troposphere [4–7].

The photoacoustic detection of NO_2 is based on the absorption of incident photons. These short pulses at $\lambda = 532$ nm obtained from a pulsed laser system act as a broadband acoustic source which help us to excite all types of the cavity modes simultaneously.

In PA measurements, the noise signals play very important roles to limit the ultimate detection sensitivity of ultralow gas concentration. These signals are produced from cell windows, electronic circuitries, external environment etc. [8–10]. However, due to the interference of the acoustic noise at the cell window, some of the excited modes of the cavity become much stronger than the others [8].

Many groups have reported the minimum noise transmission technique to design suitable acoustic filter having a length equivalent to a quarter of the acoustic wavelength for the successful elimination of undesirable noise signal [11,12]. Miklose and Lorincz [13] and Angeli *et al* [14] reported acoustic filters to record the first azimuthal mode. However, their chamber length was equal to a quarter of the acoustic wavelength. Therefore, the determination of the optimum length of the acoustic filter is very useful for calculating the actual values of noise transmission and reflection coefficients of the entire cavity. This can be achieved by incorporating two small sized cylindrical tubes which act as special filters.

The present paper reports a new design of PA resonator along with special filter to record the second-order longitudinal mode at 1390 Hz and having $Q = 30$. The special acoustic filter is meant for dumping undesirable noise signals generated by pulsed laser and cell windows. In addition, this study highlights some of the important aspects such as saturation behaviour of the PA signal, Q-factor, absorption coefficient and low-limit detection of NO_2.

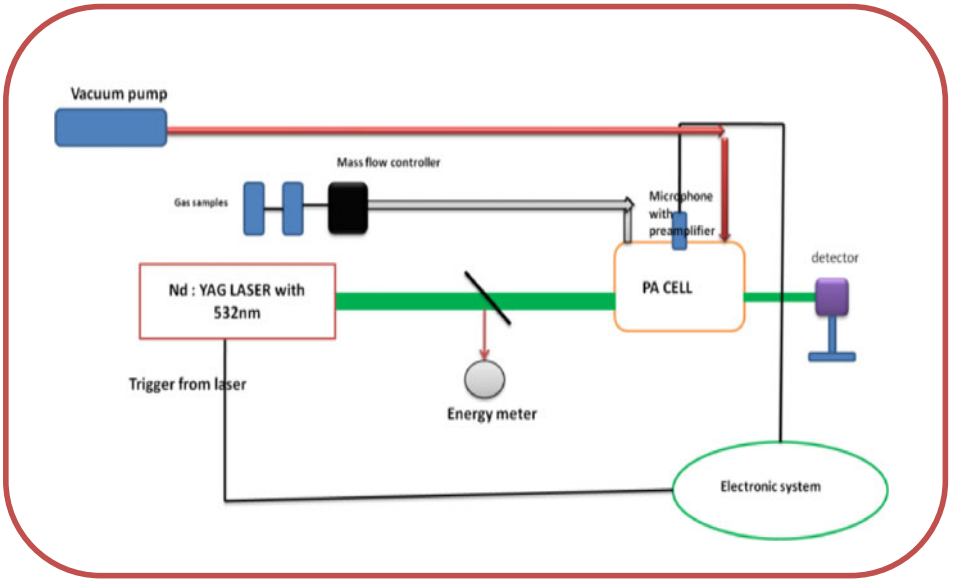

Figure 1. Experimental set-up.

2. Experimental set-up and theory

Figure 1 shows the schematic diagram of the PA experimental set-up using pulsed Nd:YAG laser system. The second harmonic of 1064 nm of Nd:YAG, i.e. 532 nm pulses having 7 ns width at a repetition rate of 10 Hz was used to excite the longitudinal modes of the cavity. A Joule energy meter (Coherent Inc.) was used to measure the laser pulse energy. To minimize the acoustic noise generated by wall absorption and windows, we have studied the generation of high level of noise with respect to beam diameter and input laser energy for air only. The value of noise increased when the beam diameter was larger than 9 mm and input laser energy was more than 15 mJ. Therefore, in our experiment the beam diameter was 7 mm. We have used PA cell with dimensions $l = 16$ cm and $r = 14.25$ mm having quartz windows and array type of microphone (BSAW-MP-241) and it was housed at the midpoint of the cell as a sensor. The cell was designed and fabricated locally.

The cell was filled with gas through the inlet using a gas handling system and the outlet was connected to the vacuum system. The strength of the microphone signal was further modified using the electronic preamplifier, Boxcar integrator (Stanford Instruments Inc., USA). The amplified PA signal was fed to the digital oscilloscope (Tektronix 2224 4-cannel) to monitor the averaged signal simultaneously. The collected data were then transferred to a PC for processing and the spectrum of NO_2 was analysed using data acquisition program developed by the lab view software. We found that the second-order longitudinal mode is excited at 1390 Hz and data acquisition time $T = 10$ mS.

The inhomogeneous wave equation of the sound pressure in the lossless cylindrical resonator was well explained by different groups [2–17].

$$\frac{\mathrm{d}_2 P(r,t)}{\mathrm{d}t^2} - c^2 \nabla^2 P(r,t) = (\gamma - 1)\frac{\mathrm{d}H(r,t)}{\mathrm{d}t}, \tag{1}$$

where c, γ and H are respectively the sound velocity, the adiabatic coefficient of the gas and the heat density deposited in the gas by light absorption.

The solution of eq. (1) is given by the series

$$P(r,t) = \sum_{n=0}^{\infty} A_{n,m} \mathrm{e}^{imw_0 t} P_n(r). \tag{2}$$

The dimensionless eigenmode distribution of the cylindrical resonator is the solution of the homogeneous wave equation which can be expressed as

$$P_n(r,t) = P_n(r)\mathrm{e}^{iw_n t}, \tag{3}$$

where w_n is the resonance frequency of the cavity resonator and $P_n(r)$ is given by

$$P_n(r) = P_{mnq}(r,\phi,z) = J_m(K_r r)\cos(K_z z)\left\{\begin{array}{c}\cos(m\phi)\\ \sin(m\phi)\end{array}\right\}, \tag{4}$$

where K_r and K_z are omponents of wave vector in radial and longitudinal directions. It is assumed that the deposited heat density directly depends on the input laser power (E). Then the amplitude A_n of the photoacoustic signal in the case of pulsed laser can be written as

$$A_n = \frac{(\gamma - 1) L f_n P_n(r_m)\alpha E}{V}, \tag{5}$$

where f_n is the normalized overlap integral which describes the effect of the spatial overlap between the propagating laser beam and the pressure distribution of the nth acoustic eigenmodes and L, V, α and γ are respectively the length, the volume of the resonator, the PA absorption coefficient of the sample and the adiabatic constant of the buffer gas. The acoustic resonant modes generated within the cylindrical cells can also be described as

$$F_{mnq} = \frac{c}{2}\left(\left(\frac{\alpha_{mn}}{R}\right)^2 + \left(\frac{q}{l}\right)^2\right)^{1/2}, \tag{6}$$

where c is the sound velocity, α_{mn} is the nth zero of the derivative of the mth Bessel function at $r = R$, where R and l represent the radius and the length of the cylinder, respectively. The normal modes are separated into longitudinal (q), radial (n) and azimuthal (m) modes.

Based on the solution of the inhomogeneous wave equation of sound pressure in the cylindrical resonator, three types of modes are present in the cavity. The first one is the longitudinal modes which solely depend on the resonator length and can directly be calculated by:

$$f_{00q} = \frac{qc}{2l}. \tag{7}$$

The form of the eigenfunction for the longitudinal mode is given by

$$P_n(r) = P_{00q}(z) = \cos(K_z z)\,. \tag{8}$$

Azimuthal and radial modes depend on the radius of the resonator and the jth zero of the derivative of the mth Bessel function divided by π. Their resonance frequencies can be calculated using the equation

$$F_{mn0} = \frac{c\alpha'_{mn}}{2\pi r} \tag{9}$$

and the corresponding eigenfunctions of mode distribution is given by

$$P_n(r) = P_{mn0}\,(r, \phi) = J_m(K_r r)\left\{\begin{array}{c}\cos(m\phi)\\ \sin(m\phi)\end{array}\right\}. \tag{10}$$

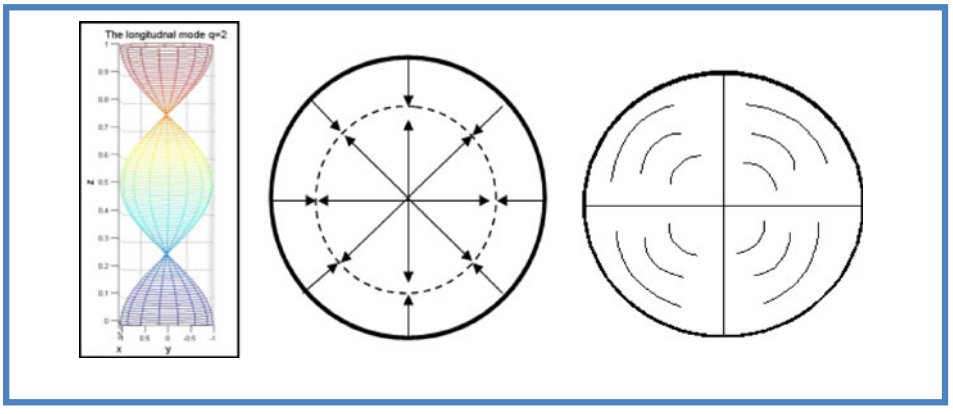

Figure 2. The schematic of the acoustic longitudinal, azimuthal and radial modes.

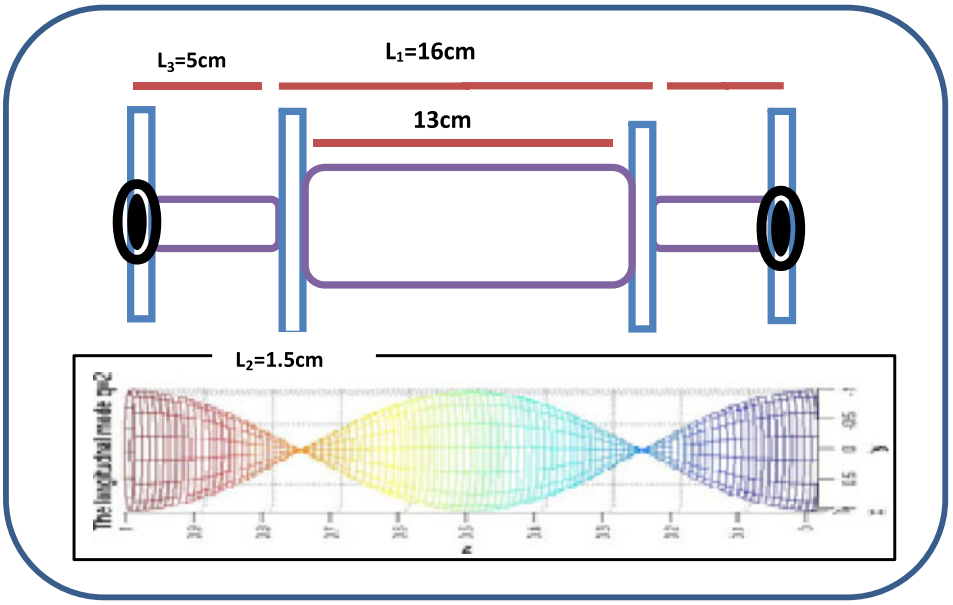

Figure 3. The resonator with specially filters and second longitudinal mode.

Figure 2 shows the schematic of the acoustic longitudinal, azimuthal and radial modes produced in the cavity due to the pulsed laser. It is well known that, if the inner surface of the cavity resonator is not homogeneous, then the generated cavity modes will decay very fast. However, the same condition is not applicable for second-order longitudinal mode which has two nodes located at the junction of the filter. The volume of the junction can also be treated as buffer volume as shown in figure 3. Consequently, the effect of inhomogeneity of the inner surface of the resonator at these two points will be very low. Therefore, these two additional tubes which extend the length of the cavity can be treated as a special filter for second-order longitudinal modes which occur at 1390 Hz frequency.

The length of the main cavity $L_1 = L + 2L_2 = 16$ cm and $R = 14.25$ mm where ($L_2 = 1.5$ cm and $R_2 = 20$ mm) along with small tube of dimension $L_3 = 5$ cm and $R_3 = 8$ mm as shown in figure 3.

The tubes L and L_2 jointly work as a low-pass filter and allow only longitudinal modes to pass and supreses other higher modes of the cavity as shown in table 1.

The whole PA system including position of filter and microphone works as a special system which is used to excite and detect second longitudinal mode.

Table 1. Longitudinal, radial and azimuthal resonance frequencies in Hz.

	1	2	3
Longitudinal	660	1320	1980
Radial	14679	26876	38974
Azimuthal	7053	11700	16094

NO_2 is excited to the $^2B_2$ state due to absorption of 532 nm and its excitation energy is lost to photoacoustic signal generation by vibrational–translational (V–T) and vibrational–vibrational (V–V) relaxations of NO_2 in collisions with air molecules. The entire model of V–T and V–V relaxation of NO_2 with N_2 and O_2 (which represent the major contribution of air components) is discussed by Kalman and Van Kesteren [17].

3. Results and discussions

Different eigenmodes of our PA cell according to eq. (3) are presented in table 1. The generated resonance frequency of the experiment is underlined. The shift of the experimental value is around 70 Hz.

Previously, we have recorded the PA signal of NO_2 in the same cavity without filter [18] where the first azimutal, first radial and 10th longitudinal acoustic modes were excited. They occupied 7050 Hz, 14650 Hz and 10350 Hz, respectively. Figure 4 shows the presence of second-order longitudinal mode excited at 1390 Hz in the same cell coupled with specially designed filter when the data acquisition time $T = 10$ ms. This is obtained by transferring the time domain signal into frequency domain using fast Fourier transform (FFT). The presence of second-order longitudinal mode is only possible when spatial noise filters are coupled to both ends of the cell. Without filter the cavity provides low limit of detection, i.e. of the order of 17.9 ppbV (parts per billion by volume) [18].

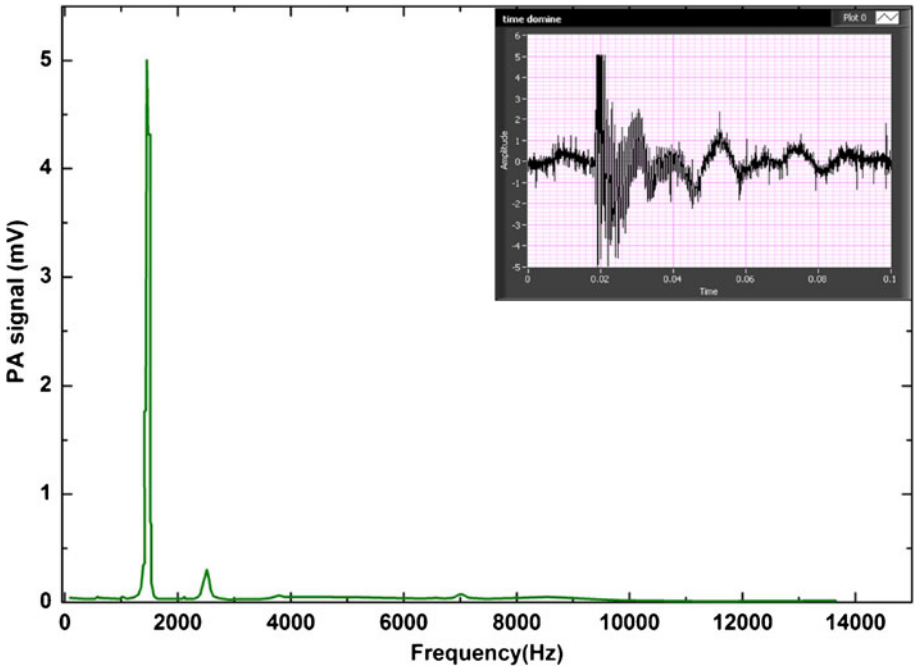

Figure 4. PA spectrum of NO_2 buffered in air at data acquisition time $T = 10$ ms.

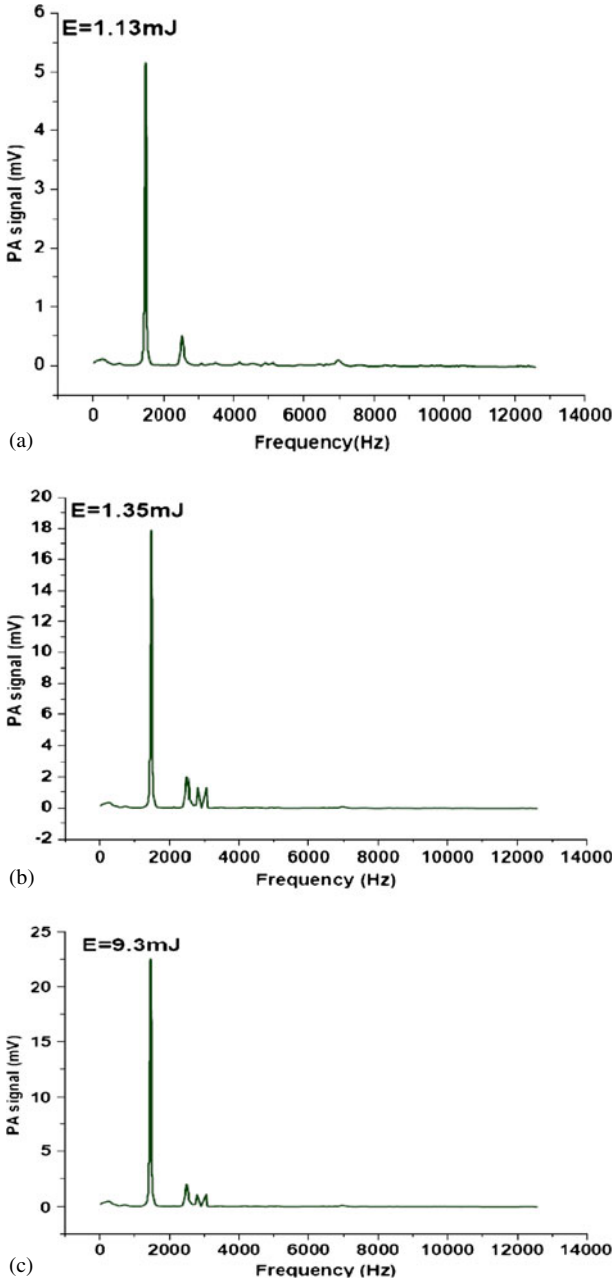

Figure 5. (**a**) PA spectrum of NO_2 buffered in air at input laser energy = 1.13 mJ, (**b**) PA spectrum of NO_2 buffered in air at input laser energy = 1.35 mJ and (**c**) PA spectrum of NO_2 buffered in air at input laser energy = 9.3 mJ.

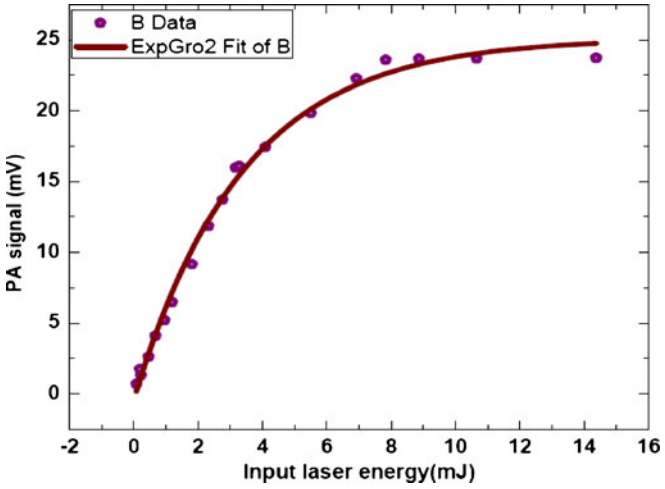

Figure 6. Dependence of PA signal on the input laser energy.

3.1 *Dependence of PA signals on input laser energy*

Figures 5a–c show the FFT of a PA signal at different input laser energies. The PA signal shows two distinct cases with respect to laser intensity. The first one is at low laser beam intensity, where the PA signal is proportional to the density of the gas squared, $(t/t_c)^2$, where t and t_c are the total de-excitation lifetime and collisional lifetime, and varies linearly with the laser beam intensity (I_0). The second case is at high laser intensity, the PA signal varies with I_0^{-1} and here the absorption saturation occurs [5,19–22].

For our system, the linear range of PA signal is found between 0.05 and 23 mV at 6 mJ input energy. The obtained results also define the actual limitation of PA technique irrespective of the concentration of gas molecules and incident laser energy. Experimental values of PA signals for the second longitudinal (0 0 2) are shown in figures 5a–c, while figure 6 clearly demonstrates the saturation behaviour.

3.2 *Q-Factor, absorption coefficient and cell set-up*

The Q-factor is defined physically as

$$Q = \frac{2\pi \text{ accumulated energy}}{\text{Energy lost over one period}} = \frac{f}{\Delta f},$$

where f_0 and Δf are the resonance frequency and the full-width at half-maximum (FWHM) of the resonance profile. The Lorentz fit of a second longitudinal mode at 1390 Hz is shown in figure 7. The experimentally estimated value of the quality factor of our PA cell is $Q = 30$.

The absorption coefficient can be calculated using the following equation:

$$\alpha = \frac{1}{l} \ln \frac{I_{\text{out}}}{I_{\text{inp}}}, \tag{11}$$

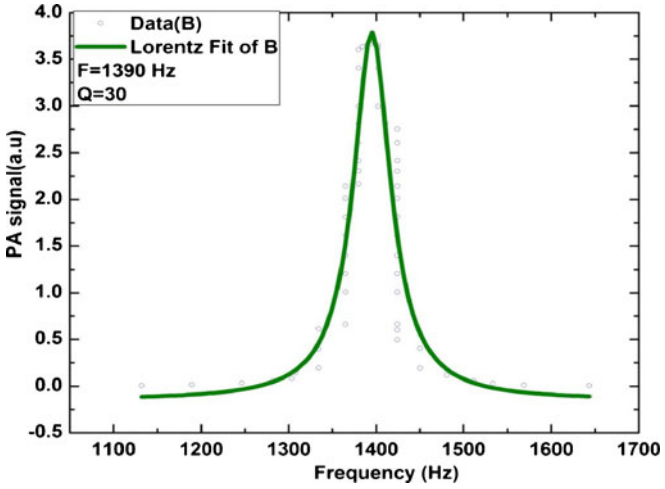

Figure 7. Lorentz fitting of the second longitudinal mode at 1390 Hz ($Q = 30$).

where I_{inp} and I_{out} represent the input and output energy of laser beam whereas L represents the length of the cell. The value of the cell set-up is 300 V cm/J which is calculated using eq. (5). We have made an attempt to find a direct relationship between the absorption coefficient and PA signal in a pulsed photoacoustic technique for the first time. It is interesting to note that two output signals are measured simultaneously, i.e. one is directly from the output of the cell and other by the microphone which yields direct relationship between the absorption coefficient and PA signal of NO_2 in a resonant PA cell coupled with special filter. The PA varies with absorption coefficient as shown in figure 8.

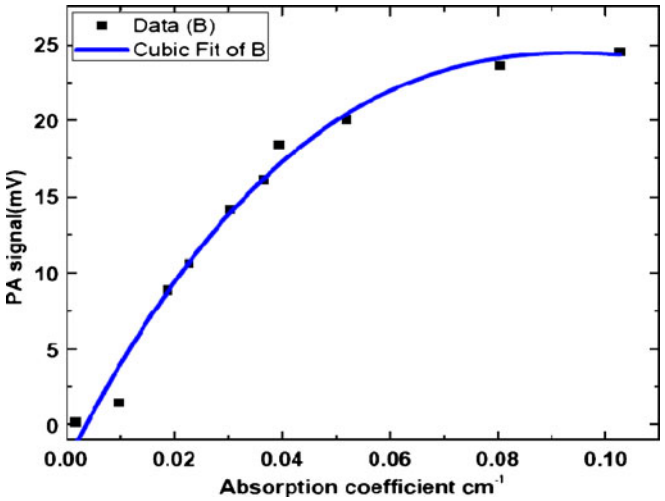

Figure 8. PA signal vs. absorption coefficient.

3.3 *Low limit of detection*

The minimum detection limit of the designed PA system can be calculated by dividing the concentration of the gas sample by the signal-to-noise ratio (SNR) [17,18]. We have recorded the background signal of the order of 0.1 μV at 7 mJ input laser energy under similar experimental condition in order to calculate the signal-to-noise ratio (SNR).

Figure 5c shows the typical strength of PA signal of NO_2 at 1 Torr pressure buffered in air with 500 Torr total pressure. As a result, we get 2000 ppmV concentration of NO_2 at 6 mJ input laser energy. The maximum recorded intensity of PA signal is of the order of 22 mV. Therefore, the estimated value of SNR of our PA system is of the order of $1*10^4$ and the corresponding minimum detection limit ($S_{\min}$) of NO_2 gas is of the order of 9 ppbV.

$$S_{\min} = \frac{2000 \text{ ppmV}}{22 * 10^4} = 9 \text{ ppbV}.$$

4. Conclusions

We have successfully designed and fabricated an efficient and versatile resonant PA cell coupled with special filters. This newly designed PA experiment works as a special system to generate second-order longitudinal modes. A systematic study of the dependence of PA signals on the incident input laser energy has also been carried out and the obtained results show the saturation behaviours of the PA signal at certain values of input laser energy. The saturation behaviour curves are also expressed in terms of the PA signal with respect to the absorption coefficient for the first time. In addition, we have achieved $Q = 30$ for the second longitudinal mode. This improvised design helps us to achieve minimum limit of detection ($S_{\min}$) of NO_2 gas of the order of 9 ppbV as compared to the previously designed cell without any filter.

Acknowledgements

Authors gratefully acknowledge the DST (SERC Project) No. SR/S2/LOP-13/03, Ministry of Science and Technology, Government of India and DRDO, Minsitry of Defence, Government of India, for partial financial support.

References

[1] A Boschetti, D Bassi, E Iacob, S Ionnatta, L Ricci and M Scotoni, *Appl. Phys. B* **74**, 273 (2002)
[2] F Yehya and A K Chaudhary, *J. Mod. Phys.* **2**, 200 (2011)
[3] M W Sigrist, Air monitoring by laser photoacoustic spectroscopy in air monitoring by spectroscopic techniques, *Chemical analysis* edited by M W Sigrist (Wiley, New York, 1994) Vol. 127

[4] J P Wolf, H J Kolsch, P Rairoux and L Woste, Remote detection of atmospheric pollutants using differential absorption techniques, *Applied spectroscopy* edited by W Demtroder and M Ingusscio (Plenum, New York, 1990) p. 435
[5] Y H Pao and C P Claspy, *Optoacoustic spectroscopy and detection* (Academic Press, New York, 1977)
[6] A K Chaudhary, G C Bhar and P Kumbhakar, *J. Quant. Spectrosc. Radiative Transfer* **98**, 157 (2006)
[7] A K Chaudhary, G C Bhar and S Das, *J. Appl. Spect.* **73**, 23 (2006)
[8] M A Gondal and M A Dastageer, *J. Environ. Sci. Health Part A* **45**, 1406 (2010)
[9] A Miklos and P Hess, *Rev. Sci. Instrum.* **72**, 1937 (2001)
[10] A Karbach and P Hess, *J. Chem. Phys.* **84**, 2945 (1986)
[11] F C Bijnen, J Reuss and F Harren, *Rev. Sci. Instrum.* **67**, 2914 (1996)
[12] L E Rinsler, A R Frey, A B Coppens and J V Sanders, *Fundamentals of acoustics* (Wiley, New York, 2001)
[13] A Miklos and A Lorincz, *Appl. Phys. B* **48**, 213 (1989)
[14] G Z Angeli, Z Bozoki, A Miklos, A Lorincz, A Thony and M W Sigrist, *Rev. Sci. Instrum.* **62**, 810 (1990)
[15] R Bartlom, M Kaucilkas and M W Sigrist, *Appl. Phys. B* **96**, 561 (2009)
[16] R C Sausa and R L Pastel, (2+2) Resonance-enhanced multiphoton ionization (REMPI) and photoacoustic (PA) spectroscopic detection of nitric oxide (NO) and nitrogen dioxide (NO_2) near 454 nm, Army Research Laboratory, TR-1418 (1997)
[17] J Kalman and H W Van Kesteren, *Appl. Phys. B* **90**, 197 (2008)
[18] F Yehya and A K Chaudhary, *Appl. Phys. B* **106**, 953 (2012)
[19] S Thomas, *Anal. Bioanal. Chem.* **384**, 1071 (2006)
[20] G A Weast, J J Barrett, D R Siebert and K V Reddy, *Rev. Sci. Instrum.* **54**, 797 (1983)
[21] A Rosencwaig, *Photoacoustics and photoacoustic spectroscopy* (John Wiley and Sons, New York, 1980)
[22] Y H Pao and C P Claspy, An investigation of the feasibility of use of laser optoacoustic detection for the detection of explosives (Case Western Reserve University, Final Report for Subcontrast 44343-v, the Aerospace Corp)